PRAMANA
— journal of
physics

Vol. 78, No. 5
May 2012
pp. 729–736

Two-particle momentum correlations in jets produced in e^+e^- annihilation at $\sqrt{s} = 60$ GeV

M E ZOMORRODIAN[1,*], F KHORRAMABADI[1], A SEPEHRI[2] and P ESLAMI[1]

[1]Department of Physics, Ferdowsi University of Mashhad, School of Sciences, 91775-1436, Mashhad, Iran
[2]Faculty of Physics, Shahid Bahonar University, P.O. Box 76175, Kerman, Iran
*Corresponding author. E-mail: zomorrod@ferdowsi.um.ac.ir

MS received 27 June 2010; accepted 11 January 2011

Abstract. The goal of this analysis is to measure the two-particle momentum correlation in jets, in the reaction $e^+e^- \rightarrow$ hadrons, to study its dependence on jet energy, and compare the results with analytical predictions of the next-to-leading log approximation (NLLA), using data collected by the AMY detector at a centre of mass energy of 60 GeV. Results are obtained for charged particles and for events with $E_{\text{c.m.}} = 60$ GeV.

Keywords. Jet correlations; two-particle momentum.

PACS No. **13.66.Bc**

1. Introduction

The evolution of jets is driven by the emission of gluons at very small transverse momenta with respect to the jet axis. The theoretical predictions, which are compared with the results of this measurement, are based on NLLA [1] calculations supplemented with the hypothesis of local parton-hadron duality (LPHD) [2]. NLLA provides an analytical description of parton shower formation, while LPHD states that the hadronization process takes place locally and, therefore, properties of partons and hadrons at the end of parton shower are closely related.

Detailed studies of jet fragmentation allow one to better understand the relative roles of perturbative parton showering and non-perturbative hadronization in shaping the main jet characteristics. Past experimental studies of inclusive distributions of particles in jets [3,4] have shown good agreement with theoretical predictions, suggesting that the perturbative QCD (PQCD) stage of jet formation must be dominant, and the role of the non-perturbative stage is reduced to converting final partons into hadrons without significantly affecting their multiplicities and momenta.

Many experimental results have been reported from high-energy experiments [5,6] which are in good agreement with PQCD prediction.

In this paper we would like to perform the complete analysis of the AMY data, based on e^+e^- annihilations at 60 GeV centre of mass energies, on inclusive momentum distributions of particles, two-particle correlations, the dependence of correlation parameters C_0, C_1, C_2 on Q, together with results obtained at CDF II detector in different Q. We show that the inclusive momentum distributions of particles, two-particle correlations and the dependence of correlation parameters C_0, C_1, C_2 on Q agree impressively well with the analytical QCD results.

2. Inclusive momentum distribution

The inclusive momentum distribution function of partons in jets $D(\xi) = \mathrm{d}N/\mathrm{d}\xi$ in NLLA is defined in terms of the variable $\xi = \ln(1/X)$ where $x = p/E_{\text{jet}}$ and p is the parton momentum.

This distribution is predicted to have a distorted Gaussian shape [7]:

$$\frac{\mathrm{d}N}{\mathrm{d}\xi} = \frac{N}{\sigma\sqrt{2\pi}}\exp\left[\frac{1}{8}l - \frac{1}{2}s\delta - \frac{1}{4}(2+l)\,\delta^2 + \frac{1}{6}s\delta^3 + \frac{1}{24}l\delta^4\right], \tag{1}$$

where $\delta = \xi - \xi_0$ and ξ_0 is the position of the maximum of the distribution. The coefficients σ, s and l are the width, skewness and kurtosis of the inclusive momentum spectrum respectively. These coefficients are calculated to next-to-leading order and depend on Q_{eff} which is defined below.

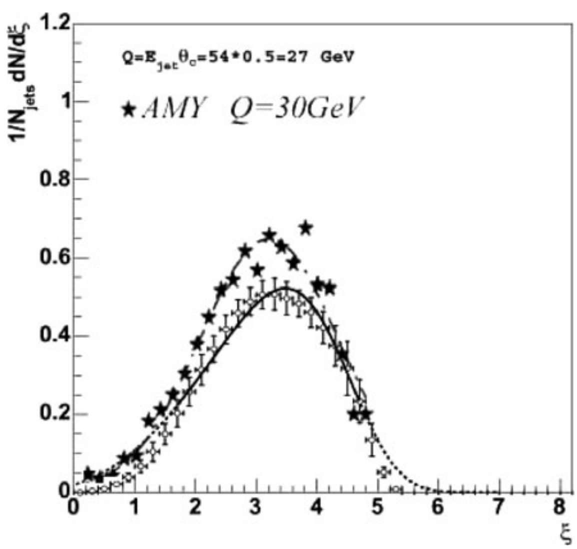

Figure 1. Inclusive momentum distributions of particles in jets. The solid curve corresponds to the fit of the CDF data, the dash–doted curve corresponds to the fit of AMY data.

The MLLA also provides a prediction for the energy evolution of the peak position of the ξ distribution [1]:

$$\xi_0 = 0.5\tau + \sqrt{c\tau} - c, \tag{2}$$

where $\tau = \ln(Q/Q_{\text{eff}})$ (Q_{eff} is the phenomenological scale and Q is the jet hardness (in this formalism, $\tau = \ln(\sqrt{s}/2Q_{\text{eff}})$) and $c = 0.2915$ (0.3190) for three (four) active flavours. ξ_0 corresponds to the peak of the inclusive momentum distribution.

By fitting eq. (1) to the ξ distribution measured in our AMY data, we find $\xi_0 = 3.220 \mp 0.03$. Furthermore, by applying eq. (2) to our data for three active flavours, we obtain $Q_{\text{eff}} = 267$ MeV. Inclusive momentum distributions of particles and the peak of the inclusive momentum distribution are shown in figure 1.

3. Two-particle momentum correlations

The correlation function was introduced in terms of the parameter $\xi = \ln(1/x) = \ln(E_{\text{jet}}/P_{\text{hadron}}) = \ln(\sqrt{s}/2P_{\text{hadron}})$ [8] and was defined as a ratio of two- and one-particle inclusive momentum distributions:

$$C(\Delta\xi_1, \Delta\xi_2) = \frac{D(\xi_1, \xi_2)}{D(\xi_1)D(\xi_2)}, \tag{3}$$

where both inclusive distributions $D(\xi) = \mathrm{d}n/\mathrm{d}\xi$ and $D(\xi_1, \xi_2) = \mathrm{d}^2n/\mathrm{d}\xi_1\mathrm{d}\xi_2$ are normalized to unity [9].

In NLLA [10], the correlation function $C(\Delta\xi_1, \Delta\xi_2)$ is predicted to be

$$C(\Delta\xi_1, \Delta\xi_2) = C_0 + C_1(\Delta\xi_1 + \Delta\xi_2) + C_2(\Delta\xi_1 - \Delta\xi_2)^2. \tag{4}$$

$\Delta\xi = \xi - \xi_0$ where ξ_0 corresponds to the peak of the inclusive momentum distribution $D(\xi)$. The parameters C_0, C_1 and C_2 also define the strength of the correlation and functions of the so-called 'jet hardness' Q and the parton shower cut-off scale Q_{eff}. C_i coefficients ($i = 0, 1, 2$) are

$$C_i = \frac{f_{\text{g}}r^2}{f_{\text{g}}r^2F_{\text{g}} + \left(1 - f_{\text{g}}\right)F_{\text{q}}}r_i^{\text{g}} + \frac{1 - f_{\text{g}}}{f_{\text{g}}r^2F_{\text{g}} + \left(1 - f_{\text{g}}\right)F_{\text{q}}}r_i^{\text{q}}, \tag{5}$$

where

$$r_0^{\text{q}} = 1.75 - \frac{0.64}{\sqrt{\tau}}, \quad r_1^{\text{q}} = \frac{1.6}{\tau^{3/2}}, \quad r_2^{\text{q}} = -\frac{2.25}{\tau^2}$$

$$r_0^{\text{g}} = 1.33 - \frac{0.28}{\sqrt{\tau}}, \quad r_1^{\text{g}} = \frac{0.7}{\tau^{3/2}}, \quad r_2^{\text{g}} = -\frac{1.0}{\tau^2}$$

$$F_{\text{q}}(\tau) = 1.75 - \frac{1.29}{\sqrt{\tau}}, \quad F_{\text{g}}(\tau) = 1.33 - \frac{0.55}{\sqrt{\tau}}, \quad \tau = \ln\frac{Q}{Q_{\text{eff}}}$$

q and g denote the correlation parameters for partons in quark jets and gluon jets, respectively.

$r = \langle n_{\text{g}}\rangle/\langle n_{\text{q}}\rangle = 9/4$ is the ratio of average multiplicities of partons in gluon and quark jets [11] using the assumption that the number of effective massless quarks $N_{\text{f}} = 3$.

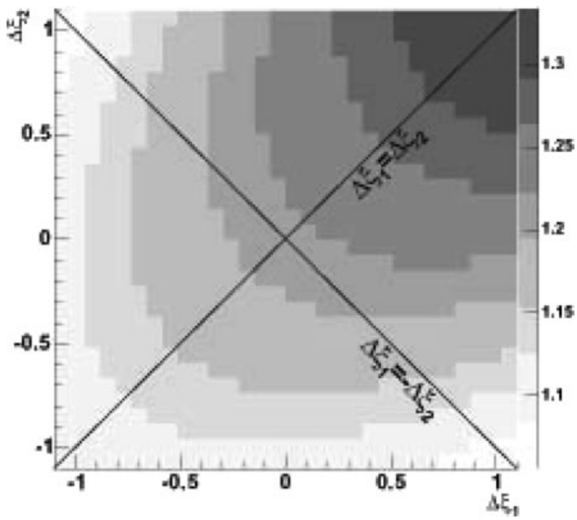

Figure 2. The NLLA parton momentum correlation function calculated for a gluon jet, $Q = 50$ GeV and $Q_{\rm eff} = 230$ MeV according to [12].

The theoretical prediction of the shape of the two-parton momentum correlation distribution function is shown in figure 2. Along the central diagonal $\xi_1 = -\Delta\xi_2$, the shape of the two-parton momentum correlation is parabolic with a maximum at $\Delta\xi_1 = \Delta\xi_2$ (figure 3). Along the central diagonal $\Delta\xi_1 = \Delta\xi_2$, the shape is linear and increasing towards larger values of ξ, i.e. lower momentum partons (figure 4). Therefore, the obvious features of the prediction are (1) the correlation should be stronger for partons with

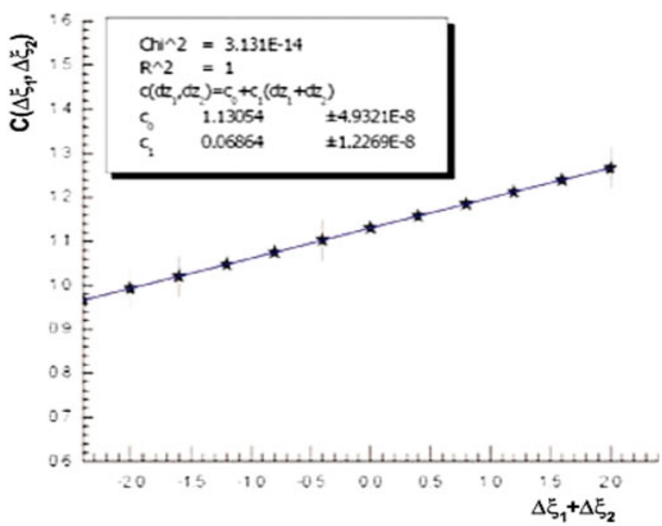

Figure 3. Two parameters C_0, C_1 obtained by fitting with eq. (4).

equal momenta ($\Delta\xi_1 = \Delta\xi_2$) and (2) the strength of this effect should increase for lower momentum partons.

The two-dimensional momentum correlation distribution is fitted according to eq. (4) with three parameters C_0, C_1 and C_2. The solid lines in figures 3 and 4 show the profiles of the fit functions. The extracted values of the fit parmeters are also indicated in figures 3 and 4.

Figures 5a and 5b show the distributions corresponding to $Q = 30$ GeV for AMY data which are compared with $Q = 27$ GeV for CDF data.

The overall qualitative agreement between the data and NLLA calculation results is very good, the data follow theoretical trends. The dashed line corresponds to the modified leading log approximation (MLLA) curve [13] and qualitatively shows the same trends. However, quantitatively the disagreement is obviously larger than that for the NLLA predictions [10].

Figure 6 shows the dependence of parameters C_0, C_1 and C_2 on jet hardness Q. Each data point corresponds to the value of one parameter measured in a particular dijet mass bin. The parameters $|C_1|$ and $|C_2|$ decrease with increasing Q. This indicates that the correlations are stronger in low-energy jets. The distributions are fit to the Fong–Webber function with Q_{eff} treated as the only free parameter. The fits are represented by solid lines. Theoretical curves for pure quark and gluon jets in the final state are also shown. We use the results of the Fong–Webber calculation [12] to fit the dependence of these parameters on jet hardness and to extract the parameter Q_{eff}. Results of the Perez–Ramos calculation are not used for the measurement of Q_{eff} because there are no corresponding analytical expressions. The value of Q_{eff} obtained from the fit of C_1 according to eq. (5) is 177 MeV. The value of Q_{eff} obtained from the fit of C_2 according to eq. (5) is 155 MeV. Accordingly, the average value of Q_{eff} extracted from the combined fit of C_1 and C_2 is 166 MeV and is consistent with Q_{eff} extracted from the fits of inclusive particle

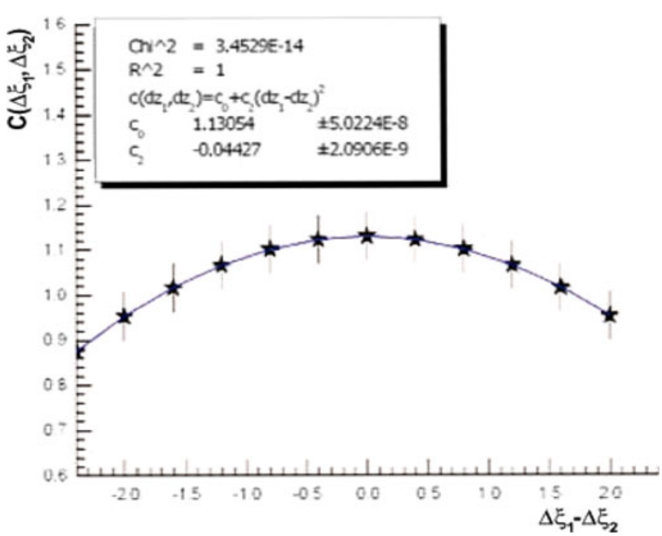

Figure 4. Two parameters C_0, C_2 obtained by fitting with eq. (4).

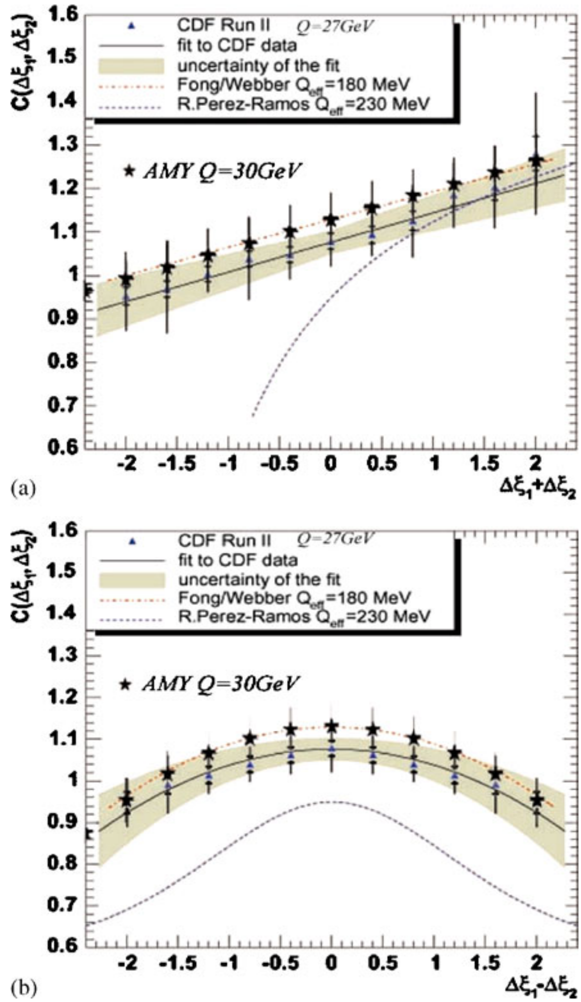

Figure 5. Two-particle momentum correlations with $Q = 30$ GeV for AMY data which are compared with $Q = 27$ GeV for CDF data. (**a**) Central diagonal profiles $\Delta\xi_1 = \Delta\xi_2$ and (**b**) central diagonal profiles $\Delta\xi_1 = -\Delta\xi_2$ of the distributions. The correlation in data is compared to that of the theory (as calculated in [12] for $Q_{\text{eff}} =$ 180 MeV and in [13] for $Q_{\text{eff}} = 230$ MeV).

momentum distributions. The parameter C_0, as opposed to C_1 and C_2, is very sensitive to the peak position ξ_0 of the inclusive momentum distribution. Theory can control only the dependence of this parameter on energy and not on its absolute value. For this reason we exclude C_0 from the measurement of Q_{eff}. A formal fit of the dependence of C_0 on Q to the theoretical function gives the value $Q_{\text{eff}} = 2$ MeV. C_0 shows very weak, if any, Q dependence, which is consistent with the theory. As a cross-check we have measured correlation distributions for pairs of tracks from opposite jets.

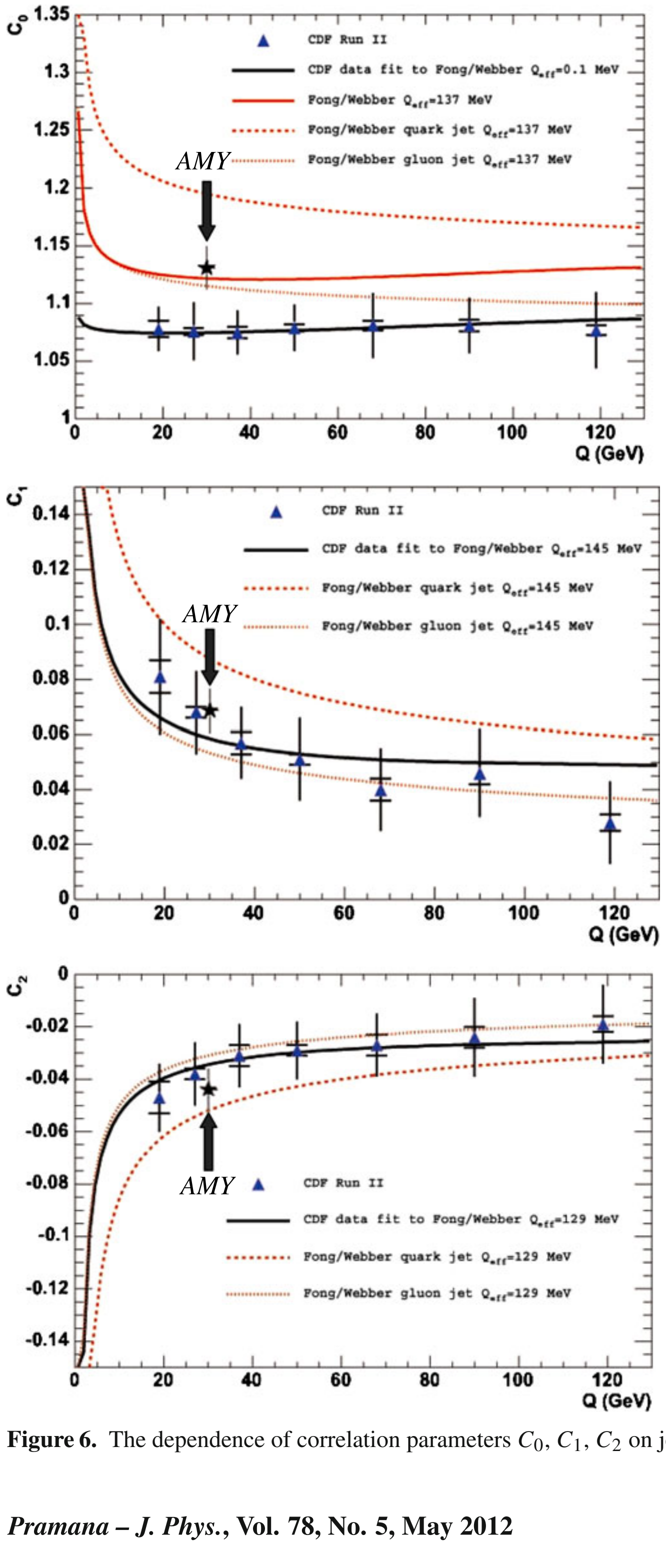

Figure 6. The dependence of correlation parameters C_0, C_1, C_2 on jet hardness.

4. Summary

The two-particle momentum correlation distributions of charged particles in jets are presented. The jets were produced in e^-e^+ collisions at a centre of mass energy of 60 GeV. The data are compared with the next-to-leading log approximation calculations combined with the hypothesis of local parton-hadron duality (LPHD). Overall, the data and the theory show the same trends over the entire range of dijet energies. The parton shower cut-off scale Q_{eff} is set equal to Λ_{QCD} and is extracted from fits of the dependence of the correlation parameters, C_1 and C_2, defining the strength of the correlation, on jet hardness Q. The average value of Q_{eff} extracted from the combined fit of C_1 and C_2 is 166 MeV and is consistent with Q_{eff} extracted from the fits of inclusive particle momentum distributions and with the results of a previous CDF measurement [4]. The modified leading log approximation predictions qualitatively show the same trends; however, the quantitative disagreement with the data is obviously larger in this case.

The results of this analysis indicate that the parton momentum correlations do survive the hadronization stage of jet fragmentation, giving further support to the hypothesis of LPHD.

Acknowledgements

This work was funded by the Vice President for Research & Technology of Ferdowsi University of Mashhad, Code 2/18432.

References

[1] Y U Dokshitzer, V Khoze, A Mueller and S Troyan, *Basics of perturbative QCD* edited by J Tran Thanh Van (Editions Frontieres, Gif-sur-Yvette, 1991)
[2] Ya I Azimov, Y U Dokshitzer, V Khoze and S Troyan, *Z. Phys.* **C27**, 65 (1985); *ibid.* **31**, 213 (1986)
[3] CDF Collaboration: T Affolder *et al*, *Phys. Rev. Lett.* **87**, 211804 (2001)
[4] CDF Collaboration: D Acosta *et al*, *Phys. Rev.* **D68**, 012003 (2003)
[5] M Schmelling, *Phys. Scr.* **51**, 683 (1995)
[6] O Biebel, *Phys. Rep.* **340**, 165 (2001)
[7] A H Mueller, in *Proc. 1981 Int. Symp. on Lepton and Photon Interactions and Energies* edited by W Pfeil (Bonn, 1981) p. 689
Y L Dokshitzer, V S Fadin and V A Khoze, *Phys. Lett.* **B115**, 242 (1982)
A H Mueller, *Nucl. Phys.* **B213**, 85 (1983); *ibid*. **B241**, 141 (1984)
[8] CDF Collaboration: D Acosta *et al*, *Phys. Rev.* **D71**, 032001 (2005)
CDF Collaboration: A Pronko, *Int. J. Mod. Phys.* **A20**, 3723 (2005)
CDF Collaboration: A Pronko, *Acta Phys. Pol.* **B36**, 451 (2005)
[9] A G Grozin, *Nucl. Phys. B (Proc. Suppl.)* **183**, 302 (2008)
[10] C Fong and B R Webber, *Nucl. Phys.* **B355**, 54 (1991)
[11] T Aaltonen, arXiv:0802.3182v3 [hep-ex], 3 April 2008
[12] C P Fong and B R Webber, *Phys. Lett.* **B229**, 289 (1989)
C P Fong and B R Webber, *Phys. Lett.* **B241**, 255 (1990)
C P Fong and B R Webber, *Nucl. Phys.* **B355**, 54 (1991)
[13] R Perez Ramos, *J. High Energy Phys.* **0606**, 019 (2006)